# Thermodynamic calculations describing the solidification of a {m,m'}-based {30Cr, 1C, 15Ta} containing alloy and microstructure Comparison with the alloy really elaborated. Part 1: {m,m'}={Ni,Co}

**Kevin Duretz[1,2], Gaël Pierson[1,2], Patrice Berthod[1,2,3]***
**[1]University of Lorraine, (FRANCE)**
**[2]Faculty of Sciences and Technologies, (FRANCE)**
**[3]Institut Jean Lamour (UMR 7198), Team 206 "Surface and Interface, Chemical Reactivity of Materials"**
**B.P. 70239, 54506 Vandoeuvre-lès-Nancy, (FRANCE)**
**E-mail : Patrice.Berthod@univ-lorraine.fr**

## ABSTRACT

This work focuses on an alloy based on Nickel and Cobalt in similar quantities, containing 30 wt.% Cr for its corrosion resistance, 1 wt.%C and 1 wt.%Ta for obtaining many TaC carbides. In a first time thermodynamic calculations were performed to describe the microstructure development during solidification and solid state cooling. In a second time the real ally was elaborated by casting from pure elements. Thermodynamic calculations predicted that solidification should start not classically by the crystallization of matrix dendrites but by TaC carbides. This was effectively verified in the real alloy with the presence of blocky TaC carbides obviously of a pro-eutectic nature. This presence of TaC in the real alloy as well as its matrix the chemical composition of which is of the same type as the high temperature austenitic matrix predicted by thermodynamic calculations show that the microstructure of the real alloy get frozen at about 1000°C during the cooling. The short temperature range of solidification determined by thermodynamic calculations did not allow the pro-eutectic carbides to migrate towards the periphery of the ingot during solidification under the decreasing electromagnetic stirring. The Vickers hardness of the real alloy is of about 30 $Hv_{30kg}$.    © 2015 Trade Science Inc. - INDIA

## KEYWORDS

Nickel;
Cobalt;
Tantalum carbides;
Thermodynamic calculations;
Solidification;
Microstructures;
Hardness.

## INTRODUCTION

Many superalloys reinforced by carbides contain simultaneously nickel and cobalt, for example for extending the temperature range of the stability of the Face Centred Cubic crystalline network of the cobalt-based matrix thanks to the presence of nickel. But either nickel or cobalt is the main element, the second one being an alloying element. Additionally alloys rich in nickel and cobalt rarely contain TaC carbides, notably with great fractions. When existing in such alloys carbides are often developed from other carbides-former elements than

tantalum.

Concerning the nickel-based alloys, if the aluminium-containing versions are maybe better known, notably as γ/γ' superalloys which feature among the best ones for high temperature applications under mechanical stresses in oxidizing atmospheres, the chromium-rich nickel-based alloys represent a high temperature alloys' family of interest. They can be still encountered in the aero-engines and hot industrial processes[1,2] (resistance against hot corrosion ensured by several tens percents of chromium) as well as in low or room temperatures applications as prosthetic dentistry[3,4] in which high mechanical properties and resistance against aqueous corrosion are required (here too favoured by chromium). Cr being a carbide-forming element the addition of carbon may lead to the development of carbides in such alloys, and with sufficient amounts of C and Cr together it is possible to obtain hard particles for achieving wear resistance[5-8].

Many applications involve chromium-rich cobalt-based alloys. These ones can be encountered in many domains, from cryogenic/ambient/body temperatures, as prosthetic dentistry[9], up to very high temperatures (e.g. aero-engines[3], industrial processes[10]), where corrosion resistance in corrosive aqueous milieus or resistance against high temperature oxidation by gases or hot corrosion by molten salts or CMAS glasses are required[11]. Many of them also contain carbon which allows the development of carbides useful for high mechanical resistance at high temperature (e.g. for combating creep deformation)[12]. Some versions especially rich in carbon and highly alloyed with carbides-former elements can be used to take benefit from the intrinsic rather high hardness of cobalt and the high hardness of carbides, for example as cutting tools[13] made of a cobalt matrix hardened with high amounts of dispersed tungsten carbides, or for Co-$W_2C$ coatings[5] for improving wear resistance of some metallic alloys.

Alloys containing, on the one hand same quantities of nickel and of cobalt, and on the other hand great quantities of tantalum carbides, seem to do not exist. This is the reason why we undertook the thermodynamic and microstructural study of an alloy based on nickel and cobalt simultaneously, containing a high chromium content to achieve high corrosion resistance at low as well as high temperature, and high contents in

carbon and tantalum – with equals atomic contents – to promote the formation of TaC carbides only.

## EXPERIMENTAL

The chemical composition of interest is basically {27Ni-27Co-30Cr-1C-15Ta}, all contents being in weight percentage. Such composition ought to lead to a {Ni,Co}-based alloy possibly with high TaC fractions and simultaneously resistant against high temperature corrosion.

This work started with preliminarily thermodynamic calculations, in order to get previsions about the development of the microstructure during solidification and solid state cooling. This was realized by using the Thermo-Calc version N software[14], with a database developed from the SSOL database[15] enriched to contain the descriptions of many of the sub-systems of the quinary {Ni, Co, Cr, C, Ta} one[16-26]. Calculations were used to predict the appearance and disappearance of the successive phases, their theoretic mass fractions and chemical compositions versus temperature, from the start of solidification down to 500°C, temperature at which it can be reasonably considered that additional solid state transformations have not time to occur, at least with atomic diffusion.

In parallel this alloy was also elaborated by foundry under 300mbars of pure Argon from pure elements (Ni, Co, Cr and Ta: Alfa Aesar, purity higher than 99.9 wt.%; and C: graphite) placed in the water-cooled copper crucible of a CELES high frequency induction furnace. The latter one was used for achieving melting, with as operating parameters: atmosphere of 300 mbars of pure Ar, voltage up to 4kV, alternative current frequency about 100kHz, (almost) isothermal stay at high temperature in the liquid state: 3 minutes. The solidification of the obtained liquid alloy was achieved by progressively lowering power. The alloy solidified in the water–cooled copper crucible of the HF furnace.

The obtained ingot, of about forty grams, was cut in two half parts. One of them was used to characterize the microstructure of the as-cast alloy over the whole ingot, in order to reveal possible heterogeneities and to take this into account for future tests or investigations. The half part under consideration was embedded in a cold resin mixture (resin CY230 + hardener HY956

*Full Paper*

from ESCIL – Lyon, France), then ground first with SiC papers from 240 to 1200 grit. Thereafter, after intermùediate ultrasonic cleaning, final polishing was performed using a textile disk enriched with 1µm alumina particles. The metallographic characterization was done using a Scanning Electron Microscopy (SEM JEOL JSM-6010LA) under an acceleration voltage of 20kV, in the Back Scattered Electrons mode (BSE) for the microstructure observations, and with the Energy Dispersion Spectrometry (EDS) apparatus for the global and pinpoint chemical composition measurements. The surface fractions of the carbides were determined by using the basic image analysis tool of the Photoshop CS software (Adobe). Hardness indentation was performed in six locations, using a Testwell Wolpert apparatus (technique: Vickers, load: 30kg).

## RESULTS AND DISCUSSION

### The main solidification and solid state transformation steps according to Thermo-Calc

Many thermodynamic calculations were performed with Thermo-Calc to better know the genesis of the microstructure. The obtained description supposes that the thermodynamic equilibrium is respected at each step, which is generally not the case for solidification and cooling of real alloys. Results (number, natures and mass fractions) are graphically given in Figure 1.

The value of liquidus temperature automatically determined by Thermo-Calc is 1333.70°C. The first crystals to appear are not metallic but carbides. These ones are the Face Centred Cubic (FCC) TaC carbides, the chemical composition of which is {93.37Ta-6.22C-0.39Cr-0.02Co-0.01Ni (in wt.%)} at this time. Their mass fraction increases during cooling, to reach 2.18% at 1245.21°C when the second solid phase starts to appear. This second phase is FCC too, and its chemical composition at its appearance, {34.77Co-31.89Ni-31.25Cr-2.03Ta-0.06C}, shows that it is the matrix. When temperature has decreased to 1244.94°C a third solid phase appears: the $M_7C_3$ carbide {86.97Cr-8.97C-3.04Co-1.02Ni and 0Ta (in wt.%)}. This one is rapidly disappears, before 1235.40°C which is solidus temperature. There, the last drop of liquid, containing {30.85Cr-28.06Ni-24.97Co-15.42Ta-0.70C (wt.%)} solidifies. The $M_7C_3$ is replaced by another
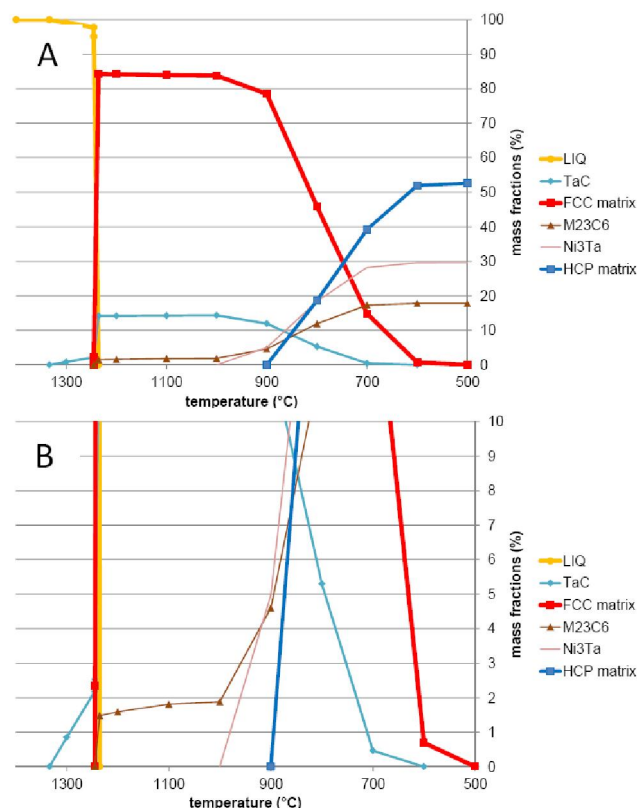


**Figure 1: Development of the microstructure of the 27Ni-27Co-30Cr-1C-15Ta alloy during solidification, according to Thermo-Calc (B: enlargement of the low mass fractions part of A)**

carbide: $M_{23}C_6$ the chemical composition is {85.12Cr-8.56Co-5.62C-0.70Ni and 0Ta (in wt.%)} at 1235.40°C. With a mass fraction of 1.59% at 1200°C and of 1.88% at 1000°C this new carbide goes on slowly developing and its growth accelerates when a $Ni_3Ta$ intermetallic phase appears and develops before 900°C. At the same time, the mass fraction of the TaC carbides, which reached 14.34% at 1000°C for example, decreases. This leads to its disappearance next to 700°C. The mass fraction of the $M_{23}C_6$ carbide finishes at 17.78% at 500°C, temperature at which the $Ni_3Ta$ phase reaches 29.59% and the second kind of matrix – the hexagonal compact one HCP appeared before 800°C – represents 52.63% of the alloy. The austenitic FCC matrix is no more present, since it disappeared at about 700°C.

### Evolution with temperature of the mass fraction and the chemical composition phase by phase

The thermodynamic calculations, even performed for a given temperature may allow anticipating the
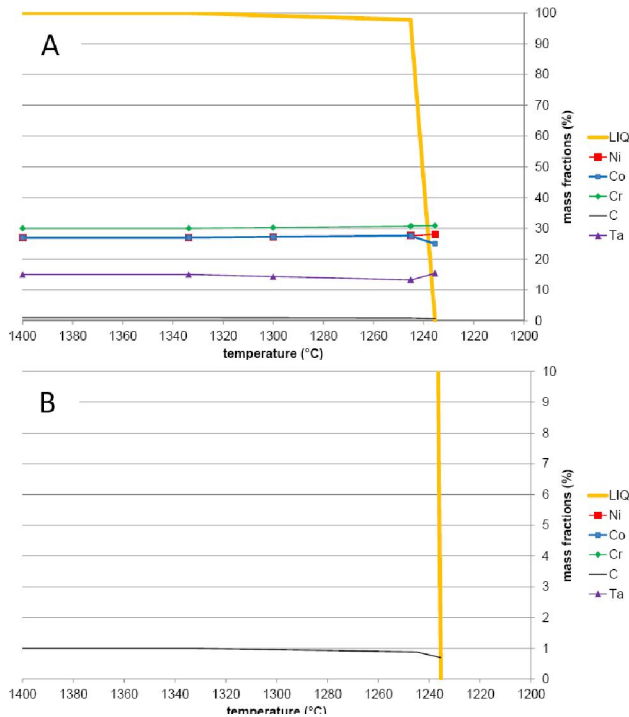
**Figure 2 : Evolution of the chemical composition of the liquid phase during the cooling until its disappearance, according to Thermo-Calc (B: enlargement of the low weight contents part of A)**
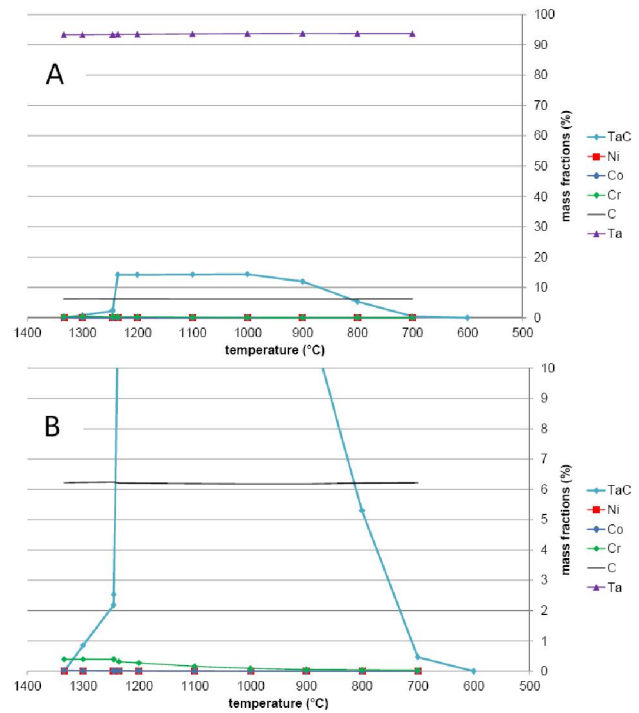


**Figure 3 : Evolution of the chemical composition of the TaC phase during the cooling until its disappearance, according to Thermo-Calc (B: enlargement of the low weight contents part of A)**

possible chemical segregations which may occur at high temperature, during solidification as well as during the cooling in solid state. Thermo-Calc was used to determine the exact temperature of appearance of each phase over the whole temperature range of solidification, and 100°C by 100°C for the solid state cooling. The results are given as graph in the following figures (from Figure 2 to Figure 7).

The chemical evolution of the liquid phase with temperature is described in Figure 2, in which the mass fraction is also recalled. The liquid phase exists alone for temperatures higher than 1333.70°C (liquidus temperature). Over this high temperatures range its chemical composition logically stays equal to the alloy's one. When the TaC phase begins to precipitates, consuming tantalum and carbon essentially, the tantalum content and carbon content in the liquid slowly decrease When the austenitic matrix starts precipitating, since this new phase contains less tantalum than the whole alloy, the tantalum content increases in the liquid, this promoting a positive tantalum segregation in the remaining melt. But when the carbides, the eutectic part of TaC carbides and the new chromium carbides, precipitate close

to the solidus temperature, the carbon content in the liquid decreases. The liquid phase totally disappears at 1235.40°C (solidus) with a chemical composition slightly enriched in chromium (30.85 against 30wt.%), tantalum (15.42 against 15 wt.%) and also in nickel (28.06 against 27%), and impoverished in cobalt (24.97 against 27 wt.%) and in carbon (0.70 against 1 wt.%).

The first solid phase to appear, the tantalum carbide TaC, starts precipitating at 1333.70°C (Figure 3). This pro-eutectic part of TaC develops until reaching 2.18% when the FCC matrix appears itself, and 2.53% at 1244.94°C at which the $M_7C_3$ also appear to disappear just after. The end of solidification, at 1235.40°C (solidus temperature), leads to a significantly greater mass fraction of TaC, with the eutectic part of this phase, to add to the pro-eutectic one. The obtained total fraction, which is equal to 14.17% at the solidus temperature, goes on slightly increasing to reach 14.34% at 1000°C, thereafter it ought decreasing and disappear before temperature reaches 600°C, according to thermodynamic calculations.

Over its whole temperature range of existence
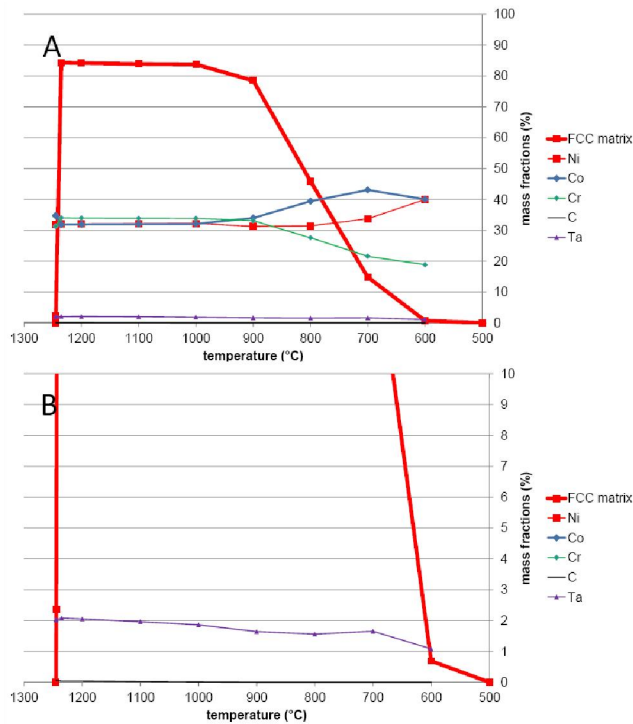
*Full Paper*



**Figure 4 : Evolution of the chemical composition of the FCC matrix during the cooling down to 500°C, according to Thermo-Calc (B: enlargement of the low weight contents part of A)**
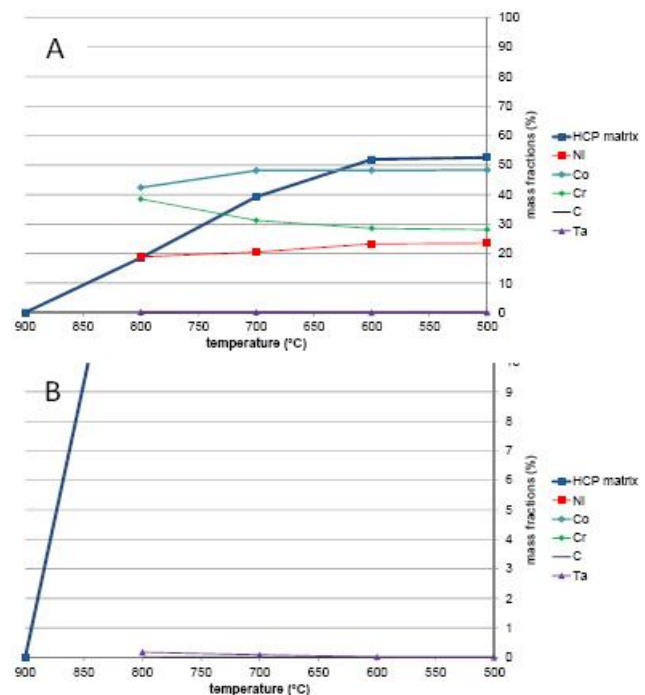


**Figure 5 : Evolution of the chemical composition of the HCP matrix phase during the cooling down to its disappearance, according to Thermo-Calc (B: enlargement of the low weight contents part of A)**

the chemical composition of the tantalum carbide is rather constant. Beside Ta and C it contains also a small quantity of chromium and its content in Cr decreases from 0.39 to 0.03 wt.% when temperature decreases from the TaC precipitation start and its disappearance.

The FCC matrix starts crystallizing at 1245.21°C (Figure 4). Its chemical composition is then rather equilibrated between Co (34.77wt.%), Ni (31.89 wt.%) and Cr (31.25 wt.%). All these contents are a little higher than in the liquid phase at the same temperature but the contents of these first crystals of matrix are poorer in carbon (0.06 wt.%) and Ta (2.03 wt.%). During the solid state cooling all these contents remain rather constant, but only before an allotropic change occurs, which progressively transforms the high temperature FCC matrix into a HCP new one. Its Ni and Co contents increase while its tantalum content decreases. The alloy arrived at temperatures slightly lower than 600°C the FCC has totally disappeared while replaced by the HCP matrix and also the intermetallic Ni$_3$Ta phase.

The chemical evolution of the HCP matrix is graphically presented in Figure 5. Shortly after its appear-

ance by solid state transformation the chemical composition of the HCP phase is rather rich in cobalt but also in chromium in chromium, for example {42.40Co – 38.51Cr – 18.90 Ni – 0.17Ta – 0.01C} at 800°C when its mass fraction is already 18.61%. Gradually as the temperature drops its chemical composition evolves and it reaches {48.39Co – 28.10Cr – 23.51 Ni – 0Ta – 0C} at 500°C. At this lowest temperature the HCP phase represents 52.63% of the alloy, the FCC matrix having disappeared just under 600°C.

The M$_{23}$C$_6$ carbides start precipitating between 1245°C and 1235°C when the alloy is partially liquid. They develops thereafter through solid state transformations, mainly during the cooling from 1000°C (their mass fraction is then only 1.88%) to 500°C (mass fractions equals to 4.60% at 900°C, 11.87% at 800°C, 17.78% at 500°C). Their chemical composition does not evolve significantly (Figure 6). One can notice only that the Co and Ni content of these Cr-rich (about 85 wt.%) carbides evolves a little, around 8.5 wt.% for cobalt, and slightly decreases from 0.70 wt.% (at the solidus temperature) to 0.19 wt.% at 500°C.
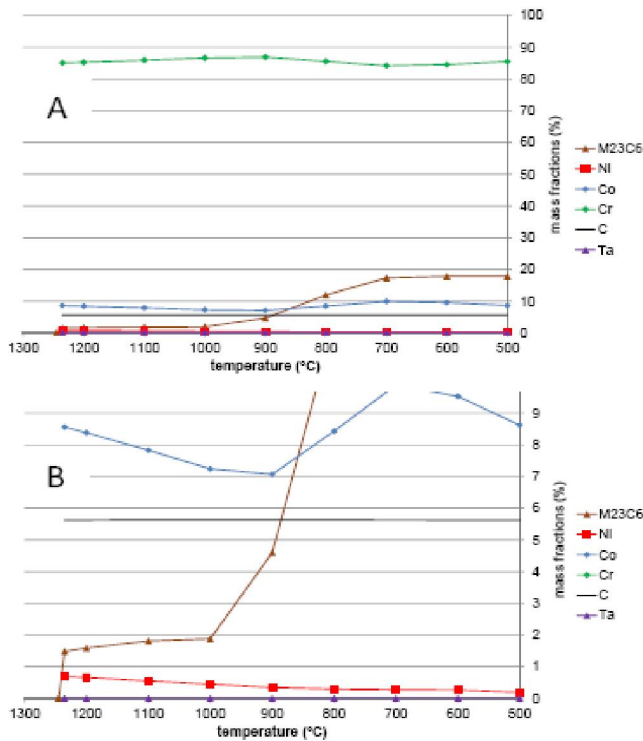
**Figure 6 : Evolution of the chemical composition of the M$_{23}$C$_6$ phase during its short existence, according to Thermo-Calc (B: enlargement of the low weight contents part of A)**

The chemical composition of the last solid phase to consider, Ni$_3$Ta (defined compound appearing between 1000 and 900°C, mass fraction of 4.98% at 900°C thereafter increasing to 29.59% at 500°C), is constant (49.32 wt.% Ni - 50.68 wt.% Ta) over its whole temperature range of existence (Figure 7).

## Microstructure of the {27Ni – 27Co – 30Cr - 1C – 15Ta} alloy really elaborated

After having prepared and weighed (about 40 grams for the mix) the different pure elements they were melted together under inert atmosphere. After solidification and metallographic preparation of half an ingot, the chemical composition was measured by EDS and the microstructure was examined by SEM/BSE, in several locations selected far from one another on the whole metallographic surface to reveal eventual chemical or microstructural heterogeneities.
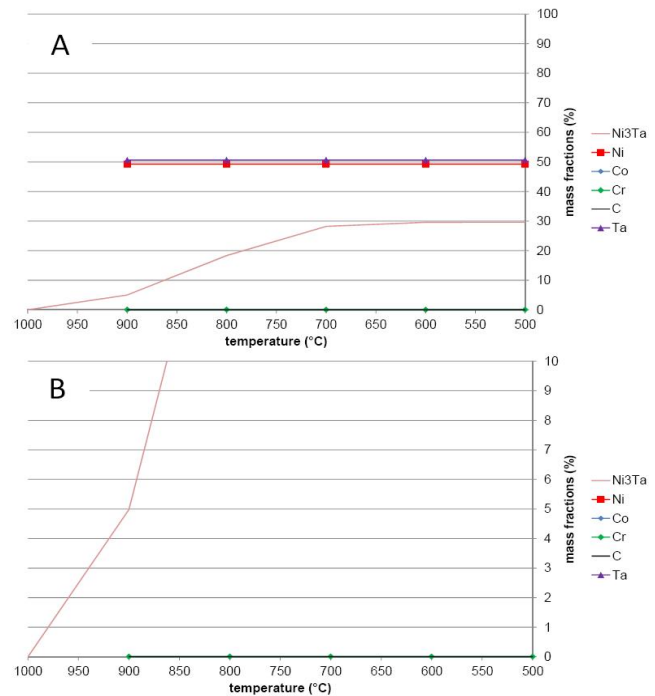


**Figure 7 : Evolution of the chemical composition of the Ni$_3$Ta intermetallic compound during its short existence, according to Thermo-Calc (B: enlargement of the low weight contents part of A)**

The chemical composition appears as being rather homogeneous. It is displayed in TABLE 1. As we can see the targeted composition is rather respected. Tnatalum appears a little too high, which is of course not possible. This classical overestimation of tantalum in alloys rich in TaC carbides is probably due to a too great exposition of these carbides on the metallographic section in electron microscopy. Concerning carbon, a too light element present in low quantity (despite its 1 wt.% which is high for carbon), EDS was not efficient enough to give a reliable value.

The microstructure of the alloy is illustrated in Figure 8 by six SEM/BSE micrographs taken in six locations chosen far from one another on the whole half ingot. One can see that the microstructure varies in term of phase surface fraction (particularly obvious for the white phase) and coarseness.

EDS pinpoint measurements were carried out in

**TABLE 1: The EDS-measured chemical composition of the real alloy**

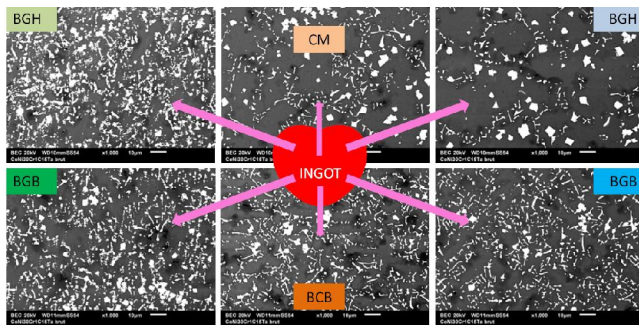| Weight percent | Ni (targeted: 27) | Co (targeted: 27) | Cr (targeted: 30) | Ta (targeted: 15) | C (targeted: 1) |
|---|---|---|---|---|---|
| Chemical composition of the alloy | 26.04 ± 1.15 | 25.90 ± 1.01 | 29.68 ± 1.17 | 18.37 ± 3.32 | Not measured |

*Full Paper*



**Figure 8: The as-cast microstructures of the studied alloy in several locations of the half part of the ingot (symbolized in red)**

rather heterogeneous though the ingot, but also that the chromium carbides do not represent a great surface fraction (only $0.36 \pm 0.29\%$) by comparison with the tantalum carbides ($12.47 \pm 4.04$ %). To finish the hardness of the alloys, in the same locations where the micrographs of Figure 8 were taken, were measured by Vickers indentation under a load of 30kg. The results, given in TABLE 5, shows that the obtained hardness (around 300) is not very high despite of the quantity of carbides.

**General commentaries**

**TABLE 2: The EDS-measured chemical composition of the matrix**

| Weight percent | Ni | Co | Cr | Ta | C |
|---|---|---|---|---|---|
| Chemical composition of the alloy | $31.95 \pm 0.23$ | $31.930 \pm 0.13$ | $31.06 \pm 0.29$ | $5.07 \pm 0.43$ | Not measured |

the matrix, in the dark particles and in the most compact white compact particles. The obtained results (TABLE 2) show that the tantalum content in matrix, which elsewhere contains similar quantities of Ni, Co and Cr, is rather high (about 5 wt.%Ta). The EDS measurements also showed that the dark particles, obviously rich in chromium, are chromium carbides and the white particles, very rich in tantalum are tantalum carbides.

The surface fractions of the carbides were measured by image analysis. The results are presented in TABLE 3 for the chromium carbides and in TABLE 4 for the tantalum carbides. This shows more quantitatively that the carbides fractions are

**TABLE 3: The surface fractions of the chromium carbides as measured by image analysis on the micrographs presented above in Figure 8**

| Localization | BGH | CM | BDH |
|---|---|---|---|
|  | BGB | BCB | BDB |
| Values (surf.%) | 0.34 | 0.34 | 0.18 |
|  | 0.92 | 0.12 | 0.24 |
| Average ± std deviation | $0.36 \pm 0.29$ | | |

**TABLE 4: The surface fractions of the tantalum carbides as measured by image analysis on the micrographs presented above in Figure 8**

| Localization | BGH | CM | BDH |
|---|---|---|---|
|  | BGB | BCB | BDB |
| Values (surf.%) | 19.47 | 10.36 | 8.47 |
|  | 14.64 | 12.01 | 9.84 |
| Average ± std deviation | $12.47 \pm 4.04$ | | |

The great weight contents in tantalum and carbon introduced in the studied alloy led to a rather dense precipitation of carbides during solidification. Many of them precipitated very early during solidification. The TaC phase was the first solid one to appear (as shown by the thermodynamic calculations), before the FCC matrix (dendritic as seen in the micrograph of the real alloy). A significant part of the TaC carbides, the most present type of carbides, is of the pro-eutectic nature, while the complementary TaC are eutectic ones, mixed with matrix. There are much less chromium carbides than TaC carbides as predicted by thermodynamic calculations (much more TaC than chromium carbides)… but only for high temperature! Indeed According to Thermo-Calc the mass fraction of TaC predominates over the $M_{23}C_6$ ones only for temperatures higher than 1000°C. This let think that the carbide repartition between TaC and chromium carbides was fixed at such high temperature, the subsequent cooling being too fast to let time to carbides to transform for a better correspondence to thermodynamic equilibria. In the same field, thermodynamic calculations showed that the FCC matrix becomes unstable under 900°C. According to the metallographic observations it did not seem that the matrix was multi-constituted. This one is not a mix of HCP and $Ni_3Ta$, since:

- first no contrast seems existing in the matrix;
- second the six EDS pinpoints analyses performed randomly in matrix all showed equivalent contents in Ni, Co and Cr (31-32 wt.%) and about

*Kevin Duretz et al.*

**TABLE 5 : The hardness values obtained in the areas where the micrographs presented above in Figure 8 were taken**

| Localization | BGH | CM | BDH |
|---|---|---|---|
| | **BGB** | **BCB** | **BDB** |
| Values (Hv30kg) | 302 | 301 | 288 |
| | 302 | 319 | 301 |

5 wt.% of Ta (TABLE 2), very different from what the HCP matrix should show ((around 40-50 mass.% of HCP containing 19-23Ni, 40-50Co, 28-40Cr and almost 0Ta, according to Thermo-Calc for 500-800°C);

- third no Ni3Ta was seen in the matrix (about 50 mass.% at 500°C according to Thermo-Calc) while a great fraction of TaC carbides was still present (they should be totally absent according to Thermo-Calc at 500°C).

The microstructure existing over 1000°C seems have been frozen during the subsequent cooling. To better specify the temperature level at which the microstructure finished to evolve during cooling the Cr and Ta contents measured by EDS in matrix have been superposed with the chemical composition of the FCC matrix according to Thermo-Calc plotted versus temperature (horizontal dotted green lines (average + one standard deviation and average - one standard deviation) for chromium in Figure 9 and horizontal dotted blue lines (average ±std deviation too) for tantalum in Figure 10). The comparison concerning chromium (Figure 9) seems showing that the chemical composition of the matrix was frozen between 900 and 850°C. The same deduction is not

possible with tantalum (Figure 10) since the EDS value remains higher than predicted by Thermo-Calc whatever the temperature.

One can compare the obtained microstructure with what was observed in previous works concerning a Co-30Cr-1C-15Ta alloy[27] and a Ni-30Cr-1C-15Ta alloy[28]. The same types of microstructures were encountered with these cobalt-based alloy and this nickel-based one: dendritic matrix, blocky pro-eutectic TaC carbides (identified thanks to Thermo-Calc too), other TaC forming a script-like eutectic with matrix, and presence of few (Co-based) or numerous (Ni-based) chromium carbides. There are also differences in The microstructural point of view: the carbide fraction seems higher in the present case than for the Ni-based and the Co-based alloy. This can be due to the outwards migration of many of the pro-eutectic TaC carbides under the electromagnetic stirring (induction heating was operating during the cooling, but with a decreasing power) in all cases. Since the te mperature range of solidification (Thermo-Calc calculations) is here lower than for the previous alloys ($T_{liquidus} - T_{solidus} = 1334 - 1235 = 99°C$ for the NiCo-based alloy against $1444 - 1296 = 148°C$ for the Co-based one[27] and $1375 - 1235 = 140°C$
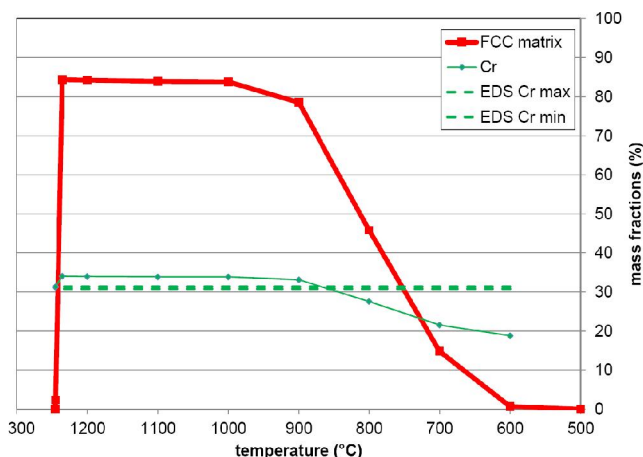


**Figure 9: Comparison of the real chromium content determined by EDS analysis in the ingot (average value ± standard deviation, two dashed horizontal green lines) with the FCC matrix chromium evolution with temperature calculated with Thermo-Calc**
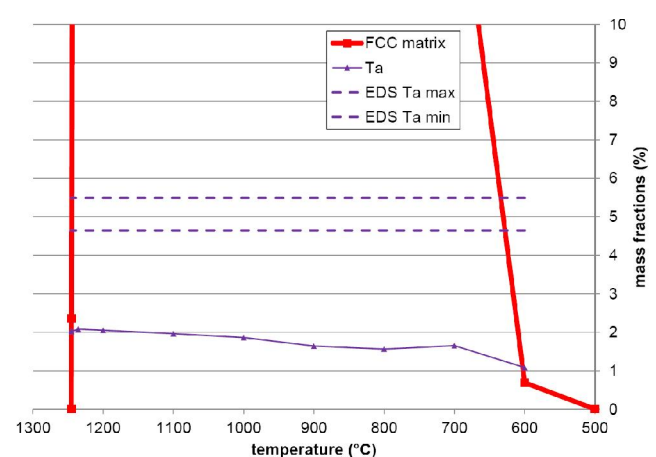


**Figure 10: Comparison of the real tantalum content determined by EDS analysis in the ingot (average value ± standard deviation, two dashed horizontal green lines) with the FCC matrix tantalum evolution with temperature calculated with Thermo-Calc**

*Full Paper*

for the Ni-based one[28]), more precisely since the temperature range of pro-eutectic TaC freedom in the melt is here lower than for the previous alloys ($T_{liquidus}$ – $T_{solidus}$ = 1334 – 1245 = 88°C for the NiCo-based alloy against 1444 – 1307 = 137°C for the Co-based one[27] and 1375 – 1272 = 103°C for the Ni-based one[28]), the time available for the growing pro-eutectic TaC to migrate towards the external surface of the semi-molten alloy was greater (the elaboration parameters were identical between the three works). For this reason there were much more blocky TaC in the periphery of the ingot for the Co-based[27] and the Ni-based[28] alloys than for the present NiCo-based alloy, which consequently contains more pro-eutectic compact TaC carbides in its internal microstructure. This helped here the hardness (average 302) to be slightly higher than the Ni-based alloy[28] (average 293) but not than the Co-based one[27] (average 436) which was helped by its intrinsically hard matrix.

## CONCLUSIONS

Thus, adding so high contents in carbon and tantalum as these 1 and 15 wt.% respectively to alloys with rather short temperature range of solidification allowed to not only develop many carbides, principally of the TaC variety which is among the most stable at high temperature, by minimizing the migration the part of these ones towards the periphery of the ingot when fusion is achieved by high frequency induction. The microstructures obtained here are much more homogeneous than previously encountered for Ni-based or Co-based alloys with similar Cr, C and Ta contents. If it appeared here that this is not really beneficial for the room temperature hardness (notably when the comparison is done with Co-based[29] and Ni-based[30] alloys highly reinforced by chromium carbides), one may wonder if the high temperature mechanical strength should be enhanced by the presence of so high TaC fractions.

## REFERENCES

[1] M.A.Engelman, C.Blechner; The New York Journal of Dentistry, **46**, 232 (**1976**).

[2] E.F.Huget, N.Dvivedi, H.E.Cosner; The Journal of the American Dental Association, **94**, 87 (**1977**).

[3] C.T.Sims, W.C.Hagel; The superalloys, John Wiley & Sons, New York, (**1972**).

[4] M.J.Donachie, S.J.Donachie; Superalloys: A Technical Guide (2nd Edition), ASM International, Materials Park, (**2002**).

[5] A.Klimpel, L.A.Dobrzanski, A.Lisiecki, D.Janicki; Journal of Materials Processing Technology, **164-165**, 1068 (**2005**).

[6] Z.T.Wang, H.H.Chen; Mocaxue Xuebao Tribology, **25**, 203 (**2005**).

[7] H.Han, S.Baba, H.Kitagawa, S.A.Suilik, K.Hasezaki, T.Kato, K.Arakawa, Y.Noda; Vacuum, **78**, 27 (**2005**).

[8] D.Zhang, X.Zhang; Surface and Coating Technology, **190**, 212 (**2005**).

[9] D.A.Bridgeport, W.A.Brandtley, P.F.Herman; Journal of Prosthodontics, **2**, 144 (**1993**).

[10] P.Berthod, J.L.Bernard, C.Liébaut; Patent WO99/16919.

[11] P.Kofstad; High Temperature Corrosion, Elsevier applied science, London, (**1988**).

[12] E.F.Bradley; Superalloys: A Technical Guide, ASM International, Metals Park, (**1988**).

[13] B.Roebuck, E.A.Almond; Int.Mater.Rev., **33**, 90 (**1988**).

[14] Thermo-Calc version N: Foundation for Computational Thermodynamics Stockholm, Sweden, Copyright, (**1993, 2000**).

[15] SGTE: Scientific Group Thermodata Europe database, update, http://www.SGTE.org, (**1992**).

[16] K.Frisk, A.F.Guillermet; Journal of Alloys and Compounds, **238**, 167 (**1996**).

[17] I.Ansara, M.Selleby; Calphad, **18**, 99 (**1994**).

[18] N.Dupin, I.Ansara; Journal of Phase Equilibria, **14**, 451 (**1993**).

[19] N.Dupin, I.Ansara; Zeitschrift für Metallkunde, **87**, 555 (**1996**).

[20] A.Fernandez Guillermet; Int.J.Thermophys., **8**, 481 (**1987**).

[21] J.O.Andersson; Int.J.Thermophys., **6**, 411 (**1985**).

[22] P.Gustafson; Carbon, **24**, 169 (**1986**).

[23] A.Fernandez Guillermet; Z.Metallkde, **78**, 700 (**1987**).

[24] J.O.Andersson; Calphad, **11**, 271 (**1987**).

[25] A.Fernandez Guillermet; Z.Metallkde., **79**, 317 (**1988**).

[26] Z.K.Liu, Y.Austin Chang; Calphad, **23**, 339 (**1999**).

[27] L.Corona, P.Berthod; Materials Science: An Indian Journal, **10(4)**, 152 (**2014**).

[28] L.Corona, P.Berthod; Materials Science: An Indian Journal, **10(5)**, 165 (**2014**).

[29] P.Berthod, E.Souaillat, O.Hestin; Materials Science: An Indian Journal, **6(4)**, 152 (**2010**).

[30] P.Berthod, O.Hestin, E.Souaillat; Materials Science: An Indian Journal, **7(1)**, 165 (**2011**).